Pol-SAR time series for soil moisture estimation under vegetation

Thomas Jagdhuber, Irena Hajnsek, Helmut Schön, Konstantinos P. Papathanassiou

Microwave and Radar Institute, German Aerospace Centre (DLR),
PO BOX 1116, 82234 Wessling, Germany,
Phone/Fax: +49-8153-28-2329 / -1449
Email: Thomas.Jagdhuber@dlr.de, Irena.Hajnsek@dlr.de,
Helmut.Schoen@dlr.de, Kostas.Papathanassiou@dlr.de

Abstract

In this paper the problem of soil moisture estimation under vegetation is investigated. Pol-SAR inversion algorithms are developed and applied on the multi-temporal AGRISAR data set from 2006 to investigate their potential and limitations over time. Modifications of the model based Freeman decomposition are used to decompose the scattering contributions and to invert the surface and dihedral scattering components for soil moisture estimation at C- and L-band. The applied decomposition approaches for agricultural land surfaces are suitable but indicate insufficiencies in modeling the volume and the dihedral components, even though some improvements due to the modifications could be shown. Finally this results in a soil moisture estimation which does not perform sufficiently well especially over the whole acquisition period.

1 Introduction

The estimation of soil moisture under vegetation by means of remote sensing is a challenging topic and has been investigated for years. The presence of vegetation posses an additional so far unsolved problem due to the gradual increase of vegetation over the growing season for the estimation of soil moisture. Dealing with soil moisture estimation on agricultural land surfaces means to take such a vegetation layer into account for the majority of the growing season. In order to overcome the vegetation disturbance on soil moisture estimation several possibilities exist to extend the parameter and observable space. In this paper SAR polarimetry is used to extend it.

The main goal is to investigate the potential of SAR polarimetry (Pol-SAR) to separate the individual scattering contributions within one resolution cell using simple canonical scattering models. Model based decompositions described in [1] - [3] are applied on C- and L-band data to invert soil moisture. In the following the modified scattering components for the decomposition, the application on experimental data and the inversion and validation are presented exemplarily over a corn field during the vegetation cycle.

2 Model based three component decomposition

As a basis for the scattering decomposition the well-known three component Freeman decomposition [2] is applied to decompose different scattering components into a surface $[T_S]$, a dihedral $[T_D]$ and a volume part $[T_V]$ [3]

$$[T_{tot}] = [T_S] + [T_D] + [T_V]$$

$$[T_{tot}] = f_s \begin{bmatrix} 1 & \beta^* & 0 \\ \beta & |\beta|^2 & 0 \\ 0 & 0 & 0 \end{bmatrix} + f_d \begin{bmatrix} |\alpha|^2 & \alpha & 0 \\ \alpha^* & 1 & 0 \\ 0 & 0 & 0 \end{bmatrix} + \frac{f_v}{4} \begin{bmatrix} 2 & 0 & 0 \\ 0 & 1 & 0 \\ 0 & 0 & 1 \end{bmatrix} . \quad (1)$$

The goal is to first decompose the individual scattering components and second to subtract the volume component from the surface and dihedral component. From these remaining components the surface soil moisture is inverted.

The surface component modeled as a Bragg surface is derived from Maxwell's equations approximated for a low frequency and for slightly rough surfaces [3]. The parameter β of the coherency matrix $[T_S]$ consists only of the Bragg coefficients (R_h, R_v) for horizontal and vertical polarization and in turn depends on the incidence angle θ and the dielectric constant of the soil ε_s, which is converted into volumetric soil moisture via a universal polynomial of Topp et al. [4]. For a more realistic formulation of a slightly rough surface the expression developed in [5] is used, introducing a cross-polarization term and a HHVV correlation which originates directly from surface roughness.

The dihedral component is modeled as a Fresnel reflection, where the soil and the perpendicular stem of a plant represent the two Fresnel planes [3]. The resulting coherency matrix $[T_D]$ is parameterized by the ratio α and the backscattering amplitude f_d, both a function of the Fresnel coefficients of the surface R_s and of the stem (e.g. trunk) R_t, depending on the incidence angle θ, the polarimetric phase difference φ and the dielectric constant of the surface ε_s and of the trunk ε_t.

The volume component in (1) is modeled as a random volume of dipoles. In order to model oriented volumes the approach of [6] is used, which models the vegetation layer with horizontally oriented, vertically oriented or randomly oriented dipoles depending on the power ratio P_r [6]:

$$P_r = 10 \cdot \log \frac{\left\langle |S_{VV}|^2 \right\rangle}{\left\langle |S_{HH}|^2 \right\rangle} \quad (2)$$

In a further approach the orientation distribution is strengthened resulting in a distribution width of $\Delta\tau = \pi / 2$. For vertical orientation the probability density function (pdf) as $p(\tau) = (1/\sqrt{2}) \sin \tau$ within $\pi/4 < \tau < 3\pi/4$ was applied, whereas for horizontal orientation the pdf as $p(\tau) = (1/\sqrt{2}) \cos \tau$ within $-\pi/4 < \tau < \pi/4$ is used to derive the following volume coherency matrices

$$\left\langle [T_V^v] \right\rangle = \frac{f_v}{30} \begin{bmatrix} 15 & 10 & 0 \\ 10 & 8 & 0 \\ 0 & 0 & 7 \end{bmatrix} \quad \left\langle [T_V^h] \right\rangle = \frac{f_v}{30} \begin{bmatrix} 15 & -10 & 0 \\ -10 & 8 & 0 \\ 0 & 0 & 7 \end{bmatrix}. \quad (3)$$

In addition to the orientation the shape of the particles ρ is also variable and is derived from [7], where the coherency matrix under assumption of a random orientation is obtained as [8]

$$\left\langle [T_V] \right\rangle = f_v \begin{bmatrix} 1+\rho & 0 & 0 \\ 0 & 1-\rho & 0 \\ 0 & 0 & 1-\rho \end{bmatrix}. \quad (4)$$

with ρ ranging from 1/3 (dipoles) to 1 (spheres).

3 Experimental results

All approaches were applied on a subset of the C- and L-band data of the west-east track acquired in the frame of the AgriSAR campaign within four months over the vegetation growing period in 2006 [9]. A European team consisting of 16 institutions performed the campaign, unique in scope and scale, to generate an image and ground database for examination and validation. The test site is located in Northern Germany and offers a variety of different soil and crop types. SAR data have been acquired by DLR's Microwave and Radar Institute's airborne E-SAR system.

3.1 Three component decompositions

Altogether five different approaches were applied:

- **Bragg** decomposition as presented in (1).
- **X-Bragg** decomposition using X-Bragg [5] instead of Bragg for surface modelling.
- **Volume 1** decomposition using (4) for the volume description.
- **Volume 2** decomposition including the volume model of [6].
- **Volume 3** decomposition incorporating the volume description of (3).

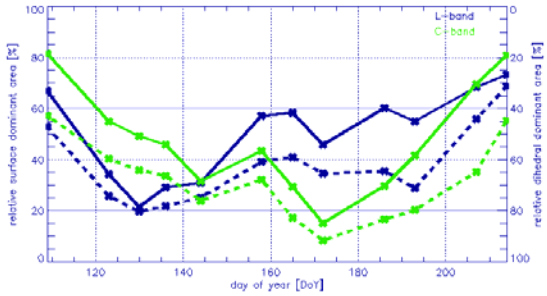

Figure 1 Percentage of surface (or dihedral) dominated points calculated using the Volume1-approach (dashed) and all other approaches (solid) at L- (green) and C-band (blue).

Figure 1 presents for the three component decomposition which mechanism is dominant at which acquisition time over the whole scene. As the shape parameter affects the decision criterion of the Volume1-approach which is not the case for all other approaches it shows for both frequencies a more distinct dihedral component at all times.

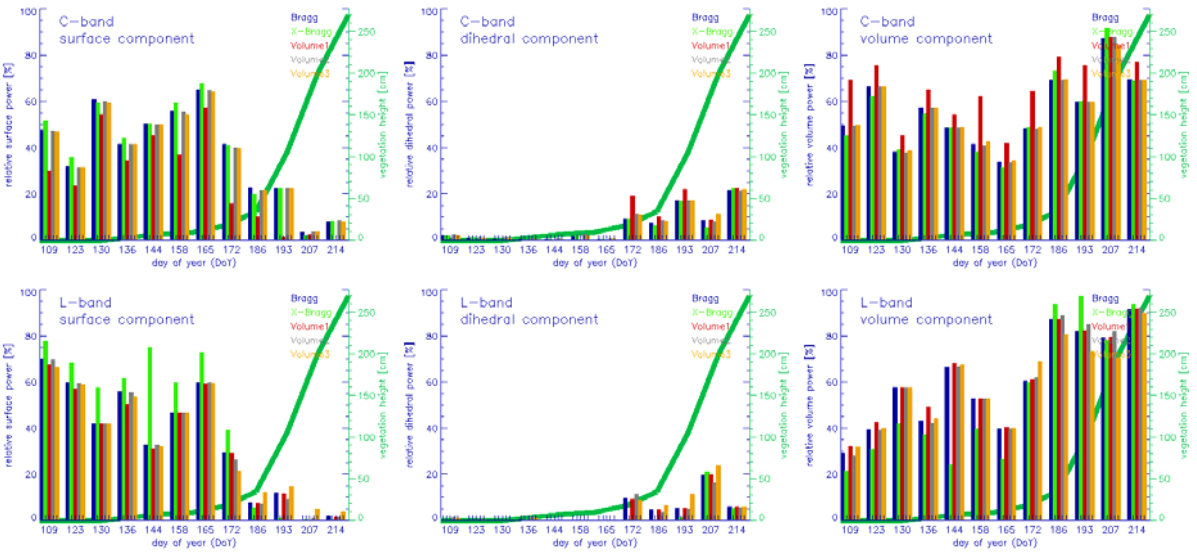

Figure 2 Relative power components (top: C-band, bottom: L-band) for the five decompositions over time exemplarily for a corn field. The powers presented are calculated for the surface, dihedral and volume components. The green curve in the background denotes the vegetation height (shown on right y-axis).

Focusing on C-band, surface scattering is dominant at the beginning of the vegetation growth period until mid of May (until day 130) and at the end of the growing season beginning from mid of July (from day 200), when most of the crops were mature, with a minimum in mid of June. Turning to L-band dihedral scattering is dominant in the early stage of the vegetation growth period in mid of May (minimum around day 130). Afterwards surface scattering is predominant from June until the end of the acquisition period (at the beginning of August) which may be due to the better penetration capabilities of L-band at a 23 cm wavelength.

To investigate the performance of the different scattering contributions (surface, dihedral, volume) over the entire growth period in both frequencies a corn field was selected (see Figure 2). The single scattering contributions are shown as relative powers, normalized to the sum of all three contributions. Comparing the three scattering components in time for C- and L-band they show in general the same behaviour driven by the vegetation growth. That means until mid of June (day 165) dihedral scattering does not exist due to the missing vegetation cover. Afterwards the situation changes when surface scattering decays and the dihedral contribution emerges until the end of the acquisition period.

The volume component reveals an increase with vegetation growth from day 165, but is also distinct in the period before without vegetation cover. It is important to note that the corn field showed a strong surface roughness before seeding and also of its seedbed. This indicates the insufficient volume description of all models leading to a misinterpretation of surface roughness induced cross-polarization as scattering of a vegetation volume. This is stronger in C- band than in L-band owing to its shorter wavelength (5 cm).

The X-Bragg approach should exhibit a better performance due to a better roughness description of the surface. This can especially be seen in L-band where the power is transferred from the volume to the surface component as compared to the other approaches. This is not the case for C-band where the roughness limit for X-Bragg (ks < 1) is violated. Looking to other approaches in detail the Volume1-approach displays a strong overestimation of the volume component over almost the whole acquisition period in C-band. Whereas in L-band this approach is consistent with almost all other approaches over time, except the X-Bragg approach for the reasons mentioned above.

3.2 Soil moisture estimation

Soil moisture was estimated over the whole acquisition period for the dominant surface and dihedral component using the five different decomposition approaches in both frequencies (C- and L-band). The validation compares values averaged from three ground measurement points at two different soil depths (0-5 cm and 5-10 cm) with the estimated soil moisture values (Figure 3). A 21 x 21 box around the sampling points leading to 441 effective looks was taken. The ground measurements are denoted by the black dashed line surrounded by a gray area showing the ±30 % interval around the respective value. Estimates outside the interval are blurred meaning not reaching the needed accuracy. In addition the vegetation height is indicated as dashed green line.

In Figure 3 on the upper plot the soil moisture at L-band retrieved from the dihedral component (in red) shows a poor performance in time. Of course only in the period when dihedral scattering is present. Soil moisture can be inverted, but the power is too low to be properly inverted. For the soil moisture values retrieved from the surface component it can be highlighted that the X-Bragg approach performs best in time. It can also be seen that for day 186 and 193 when the vegetation was growing intensively the Volume 2 – approach accounting for oriented volumes exhibits good performance.

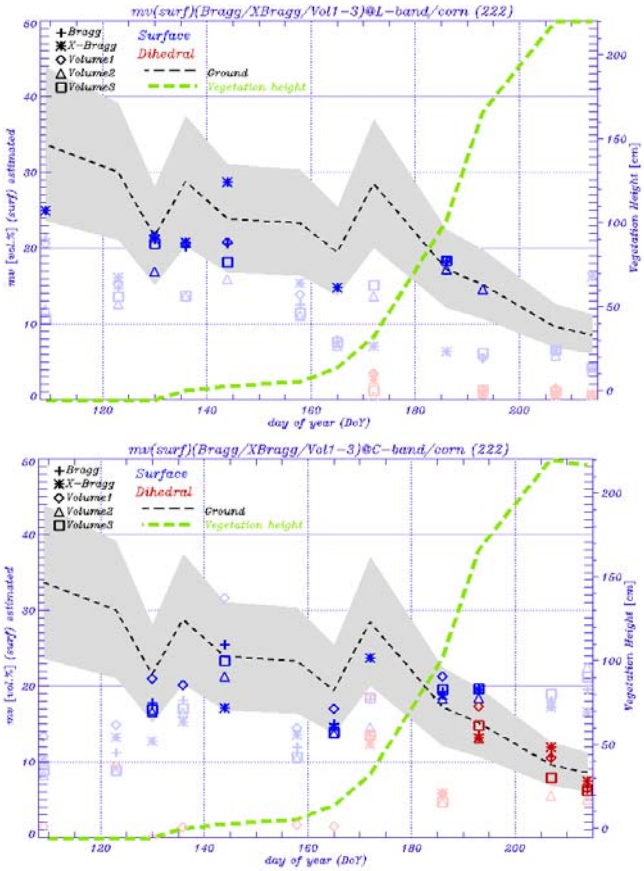

Figure 3 Comparison of mean estimated soil moisture of the corn field over time inverted from the surface (blue) and dihedral (red) scattering contribution calculated by the five approaches (top: L-band, bottom: C-band). The dashed black line corresponds to the estimated soil moisture on the ground together with its ±30 % variation region shown in gray. The green dashed line represents the vegetation height (right y-axis).

Focusing on the C- band results in the lower plot of Figure 3 the soil moisture obtained from the dihedral component shows a far better performance for the last three acqui-

sition times than for L-band, which might be induced by the higher level of the dihedral power in C- compared to L-band (see Figure 2). The results for the soil moisture estimated from the surface component have similar temporal behaviour over time compared to L-band except for the X-Bragg approach which presents a lower performance. But this is already indicated in Figure 2 where X-Bragg in C-band has an average surface power which is in the same range as all the other approaches due to the beforementioned validity range of X-Bragg ($ks < 1$). But the results for X-Bragg in C-band together with the dihedral component show good results. Finally the Volume 2 approach performs best at the times when the vegetation is strongly growing in July (day 186 and 193).

4 Summary

The modified Freeman three component decomposition of the coherency matrix was applied on the time series of the AgriSAR data set. The results shown for C- and L-band demonstrate the applicability of this decomposition on agricultural fields. The normalized scattering contributions (surface, dihedral, volume) of a corn field for the two frequencies indicate the same major trends in time, but have a different behaviour concerning the volume and roughness sensitivity. Despite the three different volume approaches (Volume1-3) the volume contribution is not modeled sufficiently well. Thus an accurate separation of surface roughness induced scattering from volume scattering is not good enough, even though the volume component was modified.
Furthermore, soil moisture was retrieved from both ground scattering components (surface, dihedral) for five different decomposition approaches in two frequencies (C- and L-band) and validated against ground measurements taken during the AgriSAR campaign in 2006. For L-band the soil moisture obtained from the dihedral contribution presented very poor results leading to the conclusion that the assumption of a specular Fresnel reflection is not compatible with natural scattering conditions at this wavelength. It is suggested that modified Fresnel coefficients, which account for scattering losses, should be applied to achieve more reasonable results [10]. For L- and C-band the soil moisture retrieved by the surface contribution indicates for most of the methods low values compared to the measured soil moisture values, caused by a weak surface component which suffers from an insufficiently modelled volume component for the before mentioned reasons. In this work the decomposition and the inversion was presented exemplarily for one crop type. During the AgriSAR campaign five different crop types were analysed for further investigations.

Acknowledgment

The authors would like to thank the AgriSAR team (Insituto Nacional de Técnica Aeroespacial (INTA), ITRES Research Limited, German Aerospace Center German Remote Sensing Data Center, Leibniz Centre for Agricultural Landscape Research (ZALF), Geo-Informatics, University Kiel, Friedrich-Schiller University, Laboratory of Hydrology and Water Management, Istituto di Studi sui Sistemi Intelligenti perl' Automazione (ISSIA), Danish Technical University, University Alicante, University Valencia, Ludwig Maximillians University, University Naples, Free University of Berlin, International Institute for Geo-Information Science and Earth Observation for their contribution to the campaign and ESA for supporting the activities. Special thank goes to Remo Bianchi and Malcolm Davidson, ESA's technical officers for their continuous support.

References

[1] Cloude, S.R. and Pottier, E.: *A Review of Target Decomposition Theorems in Radar Polarimetry*. IEEE Trans. Geosci. Remote Sensing, Vol. 34, No. 2, March 1996, pp. 498-518

[2] Freeman, A. and Durden, S.L.: *A Three-Component Scattering Model for Polarimetric SAR Data*. IEEE Trans. Geosci. Remote Sensing, Vol. 36, No. 3, May 1998, pp. 963-973

[3] Yamaguchi, Y., Yajima, Y. and Yamada, H.: *A Four Component Decomposition of POLSAR Images Based on the Coherency Matrix*. IEEE Trans. Geosci. Remote Sensing Letters, Vol. 3, No. 3, July 2006, pp. 292-296

[4] Topp, G.C., Davis, J.L. and Annan, A.P.: *Electromagnetic determination of soil water content: Measurements in coaxial transmission lines*. Water Resources Res., vol. 16, No. 3, 1980, pp.574-582

[5] Hajnsek, I., Pottier, E. and Cloude, S.R.: *Inversion of Surface Parameters From Polarimetric SAR*. IEEE Trans. Geosci. Remote Sensing, Vol. 41, No. 4, April 2003, pp. 727-744

[6] Yamaguchi,Y., Moriyama, T., Ishido, M. and Yamada, H.: *Four-Component Scattering Model for Polarimetric SAR Image Decomposition*. IEEE Trans. Geosci. Remote Sensing, Vol. 43, No. 8, 2005, pp. 1699-1706

[7] Freeman, A.: *Fitting a Two-Component Scattering model to Polarimetric SAR Data of Forests*. IEEE Trans. Geosci. Remote Sensing, Vol. 45, No. 8, 2007, pp. 2583-2592

[8] Hajnsek, I., Schön, H. and Jagdhuber, T., Papathanassiou, K.P.: *Estimation of soil moisture under vegetation using PolSAR: A Comparison of Methods*. Proc. of AgriSAR Workshop, Noordwijk, The Netherlands, October 2007, ESA-ESTEC Workshop, p. 8

[9] Hajnsek, I., Moreira, A. and Davidson, M.: *Airborne Campaigns for Pol-InSAR Applications Development*. Presentation at POLinSAR 2007, Frascati, Italy, 22-26 January 2007

[10] Lee, B.J., Khuu, V.P. and Zhang, Z.M.: *Partially Coherent Spectral Transmittance of Dielectric Thin Films with Rough Surfaces*. Journal of Thermophysics and Heat Transfer, Vol. 19, No. 3, July-September 2005, pp. 360-366